

ARTICLE

DOI: 10.1038/s42004-018-0069-0

OPEN

Kinetic control of molecular assembly on surfaces

Chiara Paris¹, Andrea Floris^{1,2}, Simon Aeschlimann^{3,4}, Julia Neff³, Felix Kling³, Angelika Kühnle³ & Lev Kantorovich¹

It is usually assumed that molecules deposited on surfaces assume the most thermodynamically stable structure. Here we show, by considering a model system of dihydroxybenzoic acid molecules on the (10.4) surface of calcite, that metastable molecular architectures may also be accessed by choosing a suitable initial state of the molecules which defines the observed transformation path. Moreover, we demonstrate that the latter is entirely controlled by kinetics rather than thermodynamics. We argue that molecules are deposited as dimers that undergo, upon increase of temperature, a series of structural transitions from clusters to ordered striped and then dense networks, and finally to a disordered structure. Combining high-resolution dynamic atomic force microscopy experiments and density-functional theory calculations, we provide a comprehensive analysis of the fundamental principles driving this sequence of transitions. Our study may open new avenues based on kinetic control as a promising strategy for achieving tailored molecular architectures on surfaces.

¹Department of Physics, King's College London, London WC2R 2LS, UK. ²School of Mathematics and Physics, University of Lincoln, Brayford Pool, Lincoln LN6 7TS, UK. ³Institute of Physical Chemistry, Johannes Gutenberg-University Mainz, Duesbergweg 10-14, 55099 Mainz, Germany. ⁴Graduate School Materials Science in Mainz, Staudingerweg 9, 55128 Mainz, Germany. Correspondence and requests for materials should be addressed to A. F. (email: afloris@lincoln.ac.uk) or to L. K. (email: lev.kantorovitch@kcl.ac.uk)

When depositing molecules on metallic and insulating surfaces, it is often assumed^{1–14} that the self-assembled structures observed are the most thermodynamically stable. However, this may not always be the case as at certain conditions, less thermodynamically stable, i.e., kinetically trapped structures, might be formed first. Therefore, using kinetics to control the formation of self-assembled structures is an approach that may open up new avenues in designing novel 2D materials. In particular, insulating substrates are of special importance for future molecular electronics, since metallic substrates cause substantial difficulties due to the appearance of leakage currents adversely affecting the devices performance. The calcite (10.4) surface represents a promising example of an insulating system, as it contains localized positively charged Ca ions and negatively charged carbonate groups CO₃, able to anchor small organic molecules strongly^{14–17}.

One of the most interesting examples demonstrating the potential of this new approach is provided¹⁷ by a system of 2,5-dihydroxybenzoic acid (DHBA) organic molecules, deposited on the calcite (10.4) surface (Fig. 1a). The molecules undergo a number of structural transitions when increasing the substrate temperature. Initially, a disordered structure consisting of clusters is formed; next, an ordered so-called striped network appears, which, upon heating the sample, is replaced by another ordered network denoted as dense¹⁷ (see Fig. 1b–e). The dense network is finally transformed into a set of disordered clusters upon further heating¹⁷. At the same time, understanding of the actual mechanisms at play, which drive the structural transformations of DHBA molecules after their deposition on the calcite surface, is missing so far. However, elucidating the role played by the thermodynamics and kinetics in determining the specific sequence of the observed networks is highly promising as it provides a route towards tailoring molecular structure formation on surfaces by kinetic control.

Here, using a combination of high-resolution dynamic atomic force microscopy (AFM) and *ab initio* density-functional theory (DFT) calculations, we provide a comprehensive explanation of the mechanisms driving the structural transformations of DHBA molecules after their deposition on the calcite surface. First, we present evidence that, under existing experimental conditions, the molecules are deposited on the surface mostly as dimers. We find that this specific molecular initial state is crucial in triggering the particular sequence and variety of the structures realized, whose relative stability is analyzed in a wide range of temperatures via thermodynamic arguments (DFT-based free energies). Second, within a fully *ab initio* approach, we calculate energy barriers associated with all evident transitions connecting the various molecular structures, allowing us to comprehensively rationalize the transition path. To the best of our knowledge, this level of theoretical analysis of the kinetics of structural transitions is unprecedented. This enables us to suggest (i) the atomistic mechanisms of dissolution and growth of each network; (ii) the composition of disordered structures along the transformation path; (iii) the rate-limiting steps in the formation of the dense network and, finally, (iv) some peculiar catalytic phenomena at play during its growth. The role played by the thermodynamics and kinetics in this complex molecular process is fully elucidated, enabling us to demonstrate that the path observed is controlled by kinetics rather than thermodynamics. Indeed, if thermodynamics establishes the most stable structure under given external conditions (e.g., coverage and temperature), kinetics provides the particular path towards this structure via a sequence of metastable states that require the highest transition rates to reach. This is highly relevant as it provides a route towards tailoring molecular structure formation on surfaces by kinetic control.

Results

Experimental results. Temperature-dependent high-resolution dynamic AFM experiments were performed to image the self-organization process of DHBA molecules sublimated on the calcite (10.4) surface.

DHBA molecules were deposited onto calcite held at 100 K and, upon stepwise heating up to 400 K, four different structural arrangements have been identified¹⁷. At low temperatures, a disordered arrangement of clusters is observed. Above 220 K, the disordered clusters start to transform into islands of a striped network, Fig. 1b. The striped network is the predominant structure in the temperature window of about 240 to 260 K, and, as illustrated in Fig. 1d, is composed of DHBA dimers formed by double hydrogen bonding of their carboxylic groups. Above a temperature of about 260 K, a continuous transition from islands of the ordered striped network to the ordered dense network islands occurs on the surface, Fig. 1c. At variance with the striped network, in the dense network the molecules are anchored to the surface through their carboxylic groups and form a monolayer consisting of upright monomers, Fig. 1e. The dense network is the dominating structure¹⁷ in the temperature range from 290 to 350 K, before it is replaced by yet another structure, formed by unordered clusters. Here, we focus on the formation of the striped network islands and the transition of the striped into the dense network. The transition process is visualized via taking a sequence of high-resolution images of the same area at room temperature over a long period of time (see Fig. 1b, c and the Supplementary Movie 1 for a complete movie of the transition). Notably, over time the dense network islands grow at locations that are different from the ones occupied by the striped network islands prior to their disappearance. Therefore, there must be a mass transfer between the two different locations, corresponding to species that appear due to dissolving striped islands and which must serve as the building material for the forming dense structures. As detailed below, the transfer is realized via mobile molecular dimers, which typically (at room temperature) move faster than the AFM scanning frequency. Hence, these species cannot be imaged at these conditions unless their diffusion rate is sufficiently decreased upon cooling the sample. AFM images of the mobile species are acquired by preparing the sample at room temperature and subsequently cooling the substrate to 185 K, as shown in Fig. 2.

As scattered individual species are clearly visible in Fig. 2 (in addition to the striped and dense islands), this suggests the co-existence of at least three structures at room temperature: striped, dense and mobile. According to the size of the scattered species being about 1 nm in diameter (measured as full width at half maximum in height profiles), we expect them to be either monomers or dimers.

As described above a series of images at room temperature (295 K) were acquired to gain a deeper insight into the striped-to-dense transformation process (see Supplementary Movie 1). In Fig. 3a–f the changes between consecutive images of the series are displayed. Striped islands dissolve and dense islands grow. After four hours, most of the striped islands vanished (over a longer period of time we expect all striped islands to dissolve). While the number of striped islands clearly decreases, the number of dense islands remains nearly constant during the observation, each increasing in size. The total area of coverage (striped plus dense islands) does not change noticeably over time ($27 \pm 5\%$). Thus, assuming that no molecules adsorb or desorb, the density of the mobile species remains also constant.

As for the dense islands, only growth is observed, indicating a larger attachment over detachment rate. Due to the glide reflection symmetry of the calcite (10.4) surface, two chiral dense

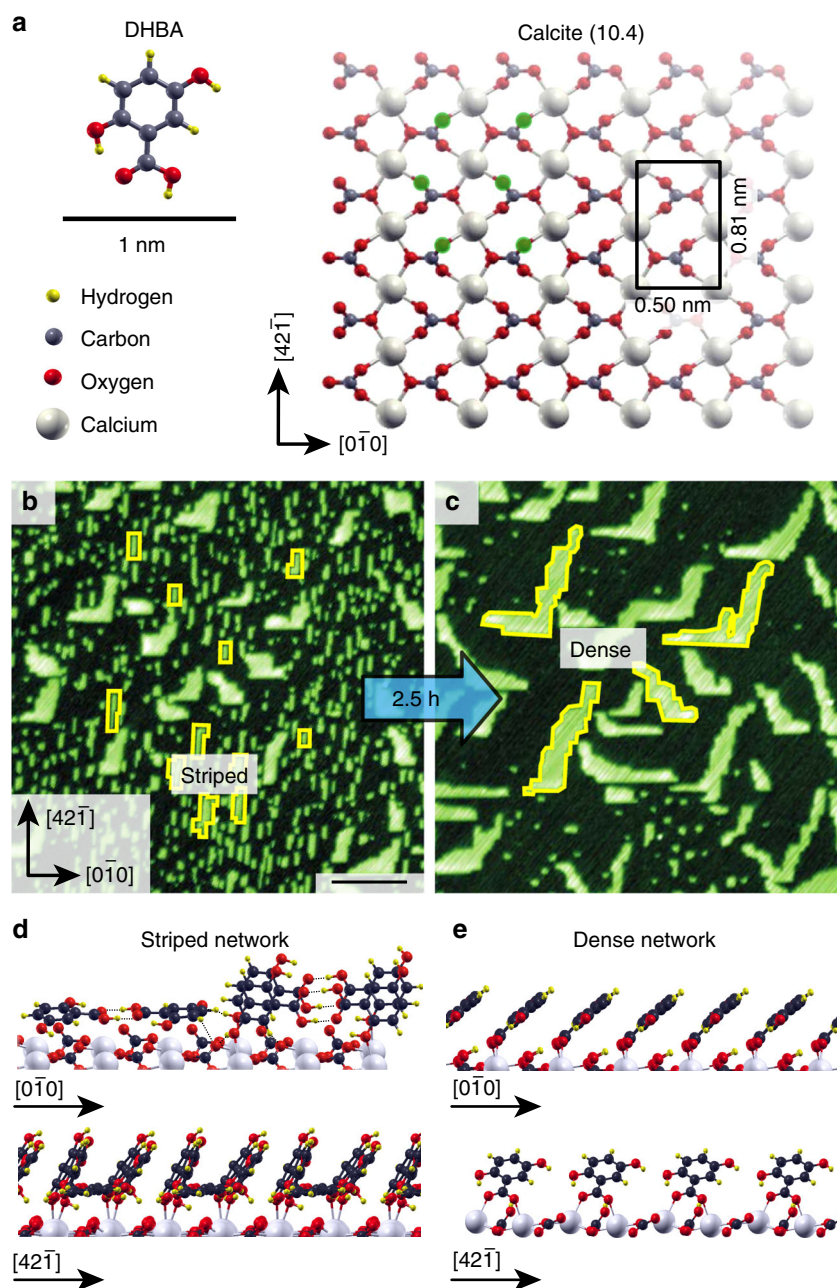


Fig. 1 Ordered networks formed by DHBA molecules on calcite. **a** DHBA molecule and top view of the (10.4) calcite surface. Green circles on some of the carbonate groups indicate the protruding oxygen atoms of the surface. **b, c** Room temperature dynamic AFM images illustrating the striped-to-dense transition. Scale bar is 100 nm. In **b** the striped network is mostly present, while in **(c)** mainly dense network islands are visible. The latter image was taken 2.5 h after the former. **d, e** Side views of the two networks obtained via DFT simulations¹⁷. **d** The striped network is formed by DHBA dimers strengthened by double hydrogen bonding of their carboxylic groups; the unit cell of this network consists of one flat and two nearly vertical dimers arranged in parallel rows. The primitive (6×1) unit cell of $3.0 \times 0.8 \text{ nm}^2$ contains six molecules. **e** In the dense network molecules are anchored to the surface through their carboxylic groups and form a monolayer of upright monomers with one molecule occupying the area of the (1×1) calcite unit cell, i.e., the molecule surface density is identical in both network structures ($2.5/\text{nm}^2$). (Images of structures used were adopted from ref. ¹⁷)

island domains exist. Dense islands growth often results in a checkmark-like form of the islands (see Fig. 3d, islands A and B).

As discussed above, a striped network island is not converted directly into a dense one at the same spot. However, the growth of the dense network islands coincides with a decrease of the striped network islands: the dense network islands “consume” the mobile species, altering the balance between these species and the striped network. This results in a preferred dissociation of the striped islands, over their growth. In other words, the disappearance of the striped network “feeds” the mobile structure while the latter

is, in turn, “consumed” at the same rate by the growing dense network.

For a detailed analysis of the growth and dissolution of the striped network, a second image series was run with the substrate kept at the somewhat lower temperature of 286 K (see Supplementary Movie 2). In Fig. 4 the changes between two consecutive images in this series are displayed. Here, we can follow the growth and dissociation of the striped network islands.

In Fig. 4b, c, an enlarged image of a nucleation and, respectively, a complete decay of a small striped island are

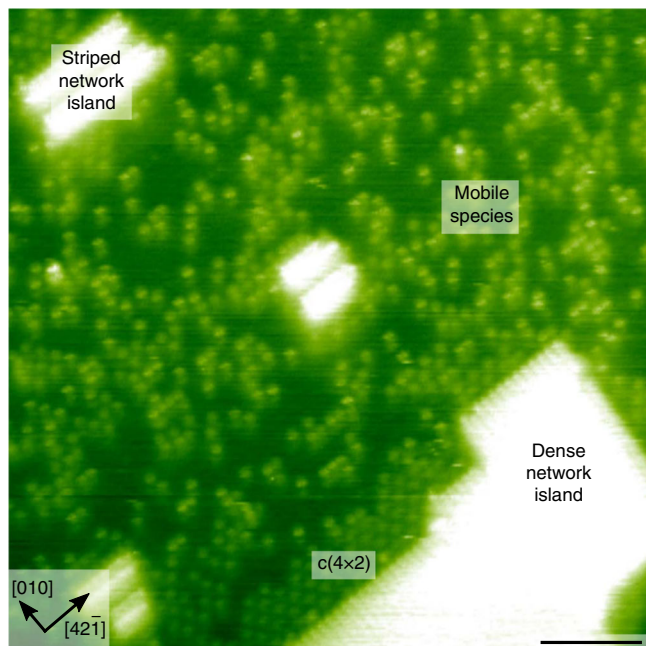


Fig. 2 Drift-corrected AFM image of DHBA on calcite. The image reveals mobile particles next to the striped and dense networks. The sample is prepared at room temperature and cooled down to 185 K. As can be seen, the area between the striped and the dense networks is occupied by species that are not observed at room temperature. Thus, these species are mobile at room temperature. Close to the dense network island, another molecule arrangement with a $c(4 \times 2)$ superstructure is visible (see Supplementary Note 7 and Supplementary Figure 19 for more information). Scale bar is 10 nm

evident. Molecules mostly attach along the $[4\bar{2}1]$ direction (Fig. 4d) and detach (Fig. 4e) at similar rate along the $[42\bar{1}]$ and $[4\bar{2}1]$ directions.

Thermodynamic consideration. The observed order in which DHBA networks appear after deposition with subsequent heating—first the striped and only then the dense network—can only be understood if we assume that initially the molecules are deposited on the surface predominantly as dimers rather than monomers. To understand this argument, let us first compare the free energies of the 2D on-surface gases of monomers and dimers with the free energies of the striped and dense networks, all calculated per molecule. In computing these free energies, vibrational and configurational entropic contributions were included in all cases (see Supplementary Note 1 for details).

The results of our calculations, Fig. 5, show that in the temperature interval of interest the 2D on-surface gas of dimers is the least stable, followed by the striped and then the dense networks, with the 2D on-surface gas of monomers being the most energetically favorable (similar results are obtained at other coverages, see Supplementary Figure 1). This analysis shows that the striped network is less favorable than the dense one, and hence its appearance before the dense network must be due to kinetic reasons (to be considered below). Moreover, it follows that if DHBA molecules were deposited as monomers, they, being the most stable, would clearly have remained as such, without forming any of the ordered structures experimentally observed. The crucial implication is that immediately after the deposition there must be a 2D gas of dimers on the surface, serving as the necessary ingredient for the subsequent formation of the striped network.

Therefore, the relevant question that one has to ask is this: why the DHBA dimers are expected to be the initial dominant species on the surface, immediately after the deposition. Several arguments justify this statement. In the gas phase, a single DHBA dimer is by 0.8 eV more stable than two separate monomers¹⁷, due to the formation of a double hydrogen bond between their carboxylic groups and to the absence of any stabilizing monomer–surface interaction. We corroborate this finding by a simple kinetic analysis (see also Supplementary Note 2 and Supplementary Figures 2 and 3), showing that in the gas phase at equilibrium dimers would significantly dominate over monomers in a very wide range of temperatures ($T = 300\text{--}1000$ K), which extends far above the experimental DHBA sublimation temperature ($T \sim 338$ K). There is yet another argument to support dimers as initial dominant molecular units. The molecules deposition is done by heating a DHBA powder, which is known¹⁸ to consist of DHBA dimers. Hence, it is natural to suggest that during the sublimation mostly dimers would be desorbed from the powder and form a vapor of dimers, since in the solid the intradimer interaction is stronger than the interaction between dimers. Therefore, mostly dimers must be adsorbed on calcite prior to formation of the ordered networks, and the very first disordered structure observed immediately after the evaporation on the surface ($T = 100\text{--}220$ K), must be a random arrangement of mostly individual dimers and their clusters. In fact, below the striped network formation temperature (220 K), the dimers mobility must be strongly suppressed.

The metastable character of the dimer structure highlighted in Fig. 5 is crucial, as it represents a necessary condition for triggering the variety of structures observed at higher temperatures.

As the temperature is increased above 220 K and dimers become sufficiently mobile, the striped network, also composed of dimers, is formed. Interestingly, even if Fig. 5 shows that this network is more favorable than the 2D on-surface gas of dimers, the dense network and the on-surface 2D monomer gas are even more stable. Why then the latter two networks are not formed directly after deposition, and instead, a much more complex sequence of structures is observed?

Kinetic consideration of structural transitions. To address the question above, it is necessary to look at the kinetics of the network formation. Three possibilities can be envisaged, with the one having the lowest overall energy barrier to be the most probable: (i) dimers dissociate into monomers, thus a 2D on-surface gas of monomers is formed; (ii) mobile dimers form striped islands, and (iii) mobile dimers form dense islands. Option (i) requires overcoming an energy barrier of 1.35 eV¹⁷, which is not feasible unless the temperature is increased significantly above room temperature. To investigate options (ii) and (iii), we need to consider the dimer mobility on the surface and the dimer attachment barriers to striped and dense islands. However, since the mobility barriers are required in both cases, they can be disregarded as we are only interested in comparing the growth rates of the two ordered networks. Also, in the DHBA attachment simulations we assumed that islands of either networks already exist, hence ignoring the associated nucleation processes. This assumption seems reasonable when comparing the growth of the two networks. In fact, even assuming that their nucleation barriers are quite diverse, the rate of the nuclei enlargement would eventually depend on how easy it is to attach a further molecule or a dimer to them. Note that one may ignore the attachment of monomers to both ordered

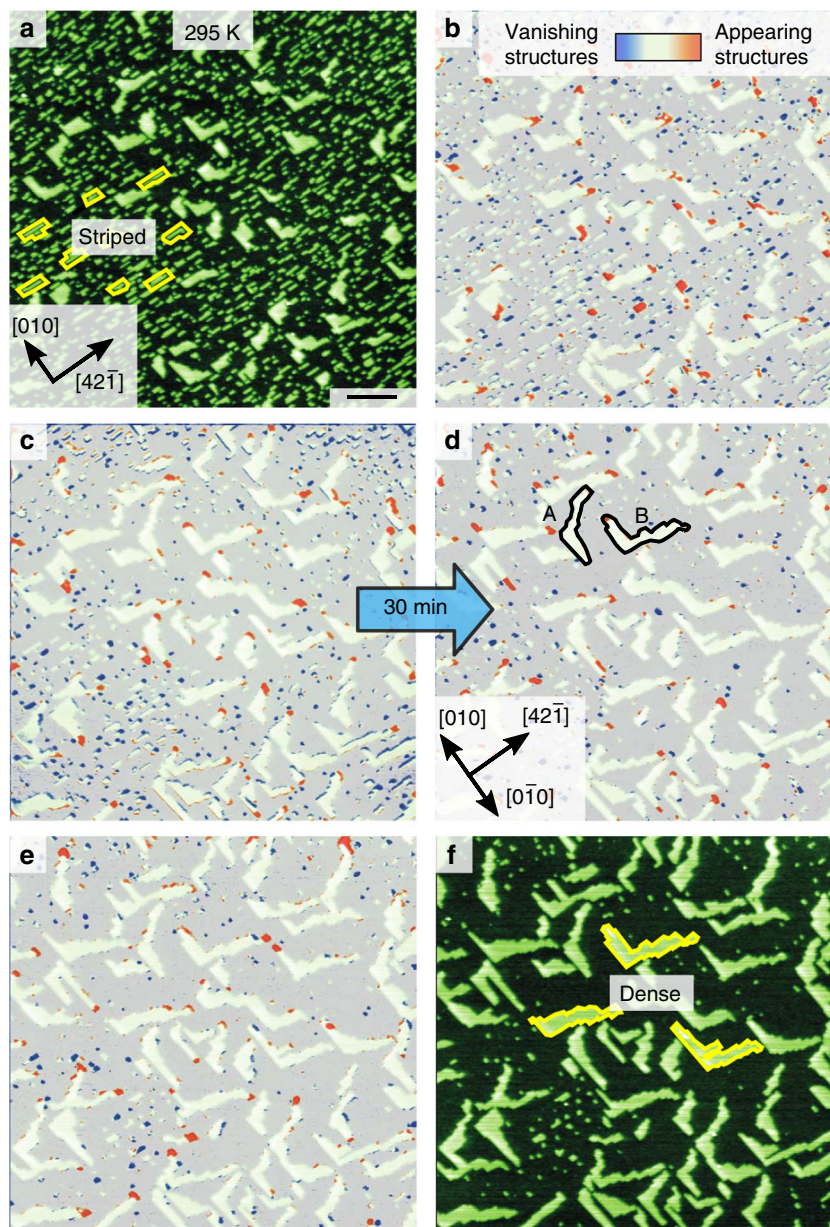


Fig. 3 An ordered selection of difference images. The AFM images were obtained during a 2.5 h series performed on a calcite surface area partially covered with DHBA molecules (see Supplementary Movie 1 for a movie of the complete series). Scale bar is 100 nm. The sample temperature is 295 K. The striped islands (some marked in **(a)**) dissolve in time, while dense islands grow (some marked in **(f)**). **b–e** Difference images are calculated by subtracting the previous image from the current one. Vanishing structures are shown with blue color, while appearing ones are in red. In **d** two chiral dense islands A and B are highlighted. Both island types grow mainly along the $[42\bar{1}]$ direction, while, in addition, islands of type A grow along $[0\bar{1}0]$ and islands of type B grow in $[010]$ direction

networks, as prior to their formation mostly dimers populate the surface.

Attachment processes to the striped network. Many attachment processes to an existing striped island are possible: a dimer can attach to an island edge, corner or kink; it can attach from various directions; the attached dimer final configuration can be either flat or upright (and in the latter case, there are two upright “sites” in the striped network unit cell). Using Nudged Elastic Band (NEB) calculations, we considered mostly attachments along the $[42\bar{1}]$ direction, as this was observed to be the main striped island growth direction in our experiments (see Fig. 4). Several monomer attachment processes were also considered.

In the very large space of possibilities analyzed, some of which are shown in Fig. 6 (see Supplementary Note 3, Supplementary Tables 1 and 2, as well as Supplementary Figures 4–9 for other processes, their barriers and molecular images), five most relevant processes c1(d), k1(d), k2(d), k3(d), and k4(d) were found. In c1(d), a flat dimer is attached to a flat-lying position at a corner with a 0.49 eV energy barrier. At the kink site the full unit cell (three dimers) can be attached in various ways, e.g., by first attaching the first (k2(d), the attachment barrier 0.59 eV) and then the second (k3(d), 0.85 eV) dimers into their appropriate vertical positions, and then adding a flat dimer (k1(d), 0.67 eV), with the process k3(d) being rate limiting. Alternatively, after attaching the first vertical dimer (k2(d)), a flat dimer can be attached next (k4(d), this is similar to k1(d) but would likely require a lower barrier

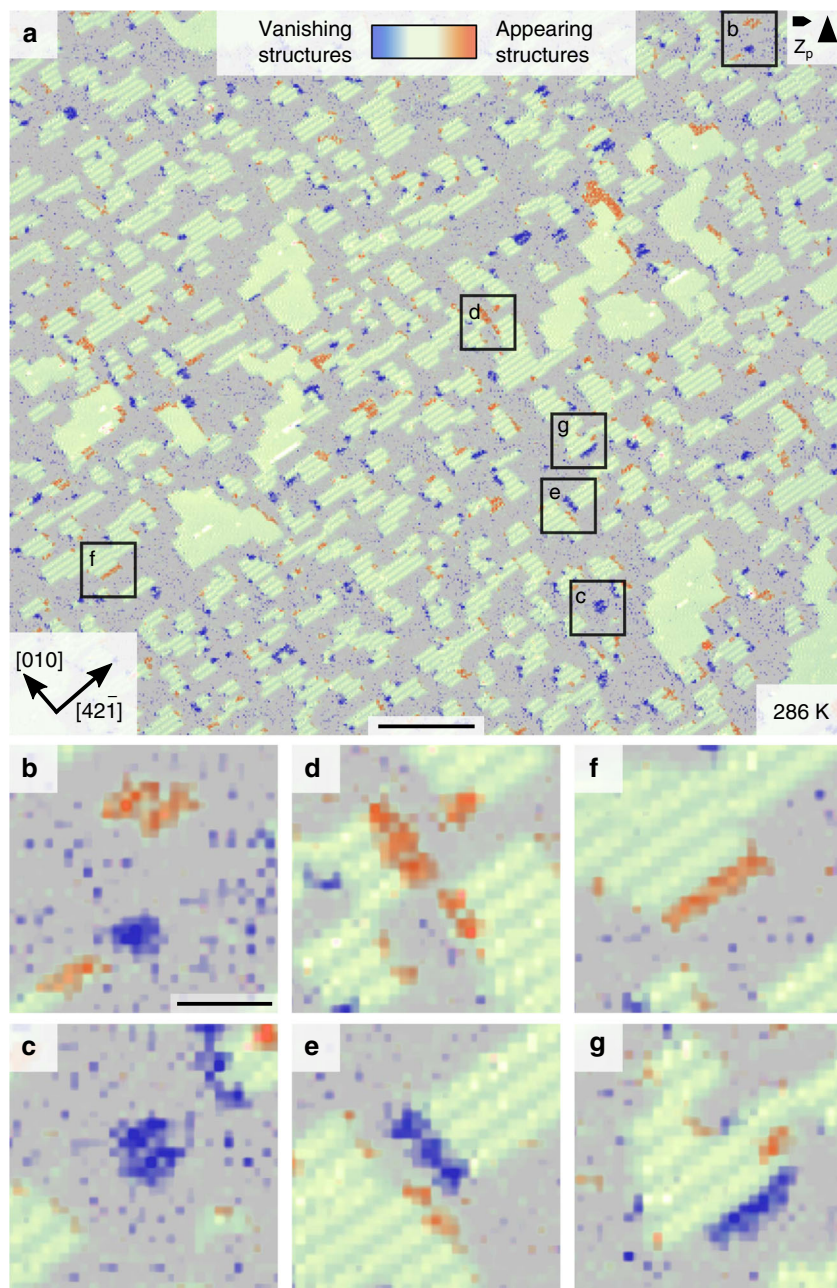


Fig. 4 Difference images from a series taken at 286 K. **a** The time difference between the two consecutive images is $\Delta t = 32$ min (see Supplementary Movie 2 corresponding to this series). Vanishing structures are marked blue and appearing structures red. Selected areas are shown in more detail underneath the main panel (**a**). They display the evolution of the striped islands in time: nucleation (**b**) and decay (**c**) of a striped island, growth (**d**) mainly along the $[42\bar{1}]$ direction and dissolution (**e**) along the $[\bar{4}21]$ and $[42\bar{1}]$ directions, growth (**f**) and dissolution (**g**) along the perpendicular $[010]$ and $[0\bar{1}0]$ directions. Scale bars are 50 nm in (**a**) and 10 nm in (**b**)

since the second vertical dimer on one side is missing), followed by the attachment of the second vertical dimer (an edge process e4(d), see Supplementary Note 3 and specifically Supplementary Figure 4), with the barrier of 0.74 eV. Both attachment routes are compared in Supplementary Figure 10; note that the second route is overall more favorable having the largest barrier by 0.11 eV lower. The attachment barriers in other processes, including those involving upright dimers at the corner sites as final states, were found to be within 0.8–1.25 eV, i.e., considerably higher.

These results indicate that the growth of the striped islands happens by moving kinks, with the two upright and a single flat dimers positions filled up in a certain order.

Finally, in all favorable processes, the final total energies are lower than the initial ones and the detachment barriers are higher than the attachment ones, ensuring stability of the striped phase over the on-surface gas of dimers.

Attachment processes to the dense network. As was mentioned, there exists a competing process after the disordered dimer network is formed upon DHBA deposition, which is associated with dimers attaching to the dense islands. Analyzing this will allow a comparison with the attachment barriers to the striped network from the on-surface gas of dimers. We will establish that the

growth (i) mainly happens at the kinks, and (ii) mostly occurs along the experimentally observed directions. In Supplementary Figure 12, we show schematically the possible attachment directions to edges and kinks of a dense island along the two main surface directions (twelve mechanisms in total, see Supplementary Figures 13–18), which we considered.

In each case we first calculated the energy difference between an initial state (a dimer placed nearby an island), and a final state (the two dimer molecules are attached to the dense island, which is made of monomers), see Supplementary Notes 5 and 6. As for edge attachments, we considered four processes. With the exception of processes k1(d) and k7(d), shown in Fig. 7, which are thermodynamically favorable, the final state in most processes was higher in energy than the initial one by 0.2–0.4 eV. This preliminary analysis allows excluding thermodynamically unfavorable processes of dense islands growth, as they would have no influence on kinetics as one would expect relatively high energy barriers. For instance, the barrier for e3(d) (see Supplementary Table 3) was found to be very high, 1.92 eV. Hence, only the two NEB kink paths k1(d) and k7(d) are meaningful, with calculated energy barriers of 0.91 and 0.71 eV, respectively, much lower than

for the edge attachment. Therefore, we can conclude that the growth of the dense islands must occur mostly by the kink mechanism.

In k1(d) and k7(d) processes, a dimer first approaches the dense network, then it dissociates, and finally the two monomers attach to the island one after another, next to each other (see Supplementary Figure 15). The monomers change their orientation on the surface as required when attaching. Importantly, the growth mechanisms associated with k1(d) and k7(d) correspond to the experimentally observed dense island growth along the $[42\bar{1}]$ and $[010]$ directions, respectively (see Fig. 3d, where the shape of island B assumes precisely these main growth directions). Due to the glide symmetry of calcite, there will be domains growing along the $[42\bar{1}]$ and $[0\bar{1}0]$ directions as well, also in agreement with experimental observations (Fig. 3d, island A).

Interestingly, the dissociation barrier of the dimer in proximity to the dense network (between 0.71 and 0.91 eV) is much lower than the one for a free dimer on the surface (1.35 eV). This “network-assisted” dimer dissociation is explained by the formation of inter-molecular interactions inside the dense network structure¹⁷, which strongly reduce the cost of breaking two intradimer hydrogen bonds. Thus, we conclude, a specific catalytic mechanism is at work for dissociating the dimers in the presence of the dense network.

In conclusion, we are now able to answer the question posed above, related to the three possible paths for the system of the on-surface gas of dimers to take. The energy barriers for the dimer dissociation (1.35 eV), the dimer attachment to the dense network (0.71–0.91 eV) and to the striped network (0.49–0.74 eV) enable us to understand that the striped network is the first to form: this route requires overall the smallest energy barriers. Therefore, the appearance of the striped network is governed by kinetics rather than thermodynamics of the system: this metastable network is formed before a more stable dense network, because it is easier to reach at the given experimental conditions.

Striped-to-dense network transition. Next, in order to understand the formation of the second, dense network, we analyze the attachment mechanisms to the dense islands (attachment of dimers have already been considered above). We first have to understand whether monomers or dimers, serving as the building material for the dense network, are mostly become available on the surface after the striped islands dissolution. Hence, we compare the barriers required for both dimers and monomers to detach from the striped islands.

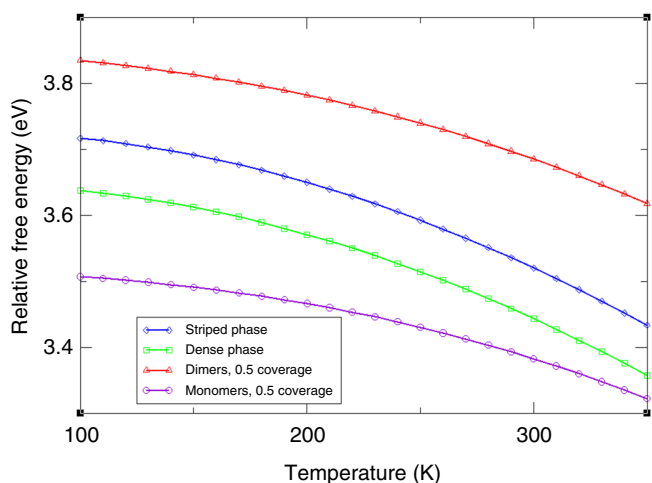


Fig. 5 Calculated free energies of different structures of DHBA molecules on calcite. Shown are the free energies (per molecule) of the 2D on-surface gases of DHBA monomers and dimers ($\theta_M = 0.5$ monomer coverage, corresponding to a molecular density of 1.25 monomers/nm²), and of the ordered striped and dense networks

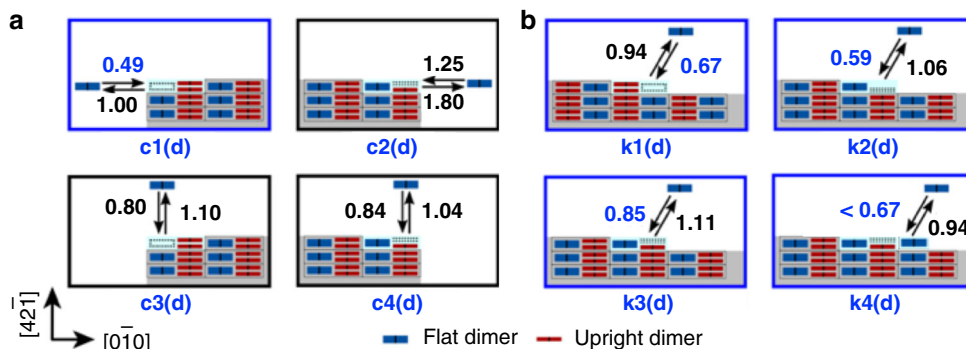


Fig. 6 Dimer attachment and detachment processes at a striped island. Schematics show a selection of such processes (a) at a corner and (b) at a kink of the island. Red and blue boxes correspond to upright and flat dimers, respectively. The calculated energy barriers (in eV) are also indicated next to the arrows associated with them, with the most favorable ones highlighted in blue. The labeling is such that, e.g., c2(d) process corresponds to the attachment at a corner (marked “c”), where the moving unit is a dimer (“d”); edge and kink are labeled with “e” and “k”, respectively. Attaching a dimer at a vacant site (not shown, see Supplementary Note 3) at a step edge requires very small energy barriers, as anticipated

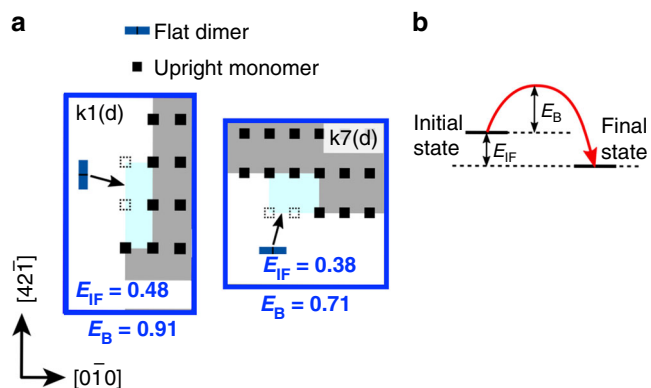


Fig. 7 Selected dimer attachment processes at a kink of the dense island. **a** Two energetically favorable processes are shown for two surface step directions, k1(d) and k7(d); **b** energy diagram defining the energies given in **a**, E_B (energy barrier) and E_{IF} . The latter corresponds to the difference between the initial (a dimer is placed next to the island) and final (the two molecules from the dimer are attached to the island) states of each process (the larger the more favorable). The arrows point out the directions of attachment of the species to the network

Of all processes considered (see Supplementary Note 3), the reverse paths in processes c1(d), k1(d) and k4(d) of Fig. 6 has the lowest detachment barriers (1.00 and 0.94 eV). The higher detachment than attachment barriers can be ascribed to breaking π -stacking interactions of the removed dimer with the neighboring upright dimers. At the same time, it is much more difficult to remove a monomer from the striped islands (energy barriers are 1.10–1.57 eV), since the intradimer hydrogen bonds must break for releasing the first monomer of each dimer. Moreover, when comparing with the dimer detachment process, two consecutive detachments of monomers from the striped islands need to happen, leading to an even lower overall rate (see Supplementary Note 4 and Supplementary Figure 11). Hence, the mobile species introduced in Section Results, which supply the material for building the dense network, are to be mostly dimers. Therefore, the attachments of dimers to the dense islands, already considered in Section Experimental methods, are entirely sufficient for understanding the growth of the dense network.

Finally, we note that attachments of dimers to the dense network have a larger rate (lower barriers, 0.71–0.91 eV) than their dissociation on the surface (1.35 eV), i.e., one can safely assume that dimers, after leaving the striped islands, may diffuse to dense islands without dissociation.

Discussion

The energy barriers considered above enable us to understand the underlying mechanisms of the observed transitions. Figure 8 summarizes our findings from two perspectives: (a) temperature and (b) free energy.

The initial preparation of the system (process 1 \rightarrow 2 \rightarrow 3), whereby the surface becomes mostly populated by DHBA dimers and their clusters, appears to be crucial. At temperatures below 224 K, when the mobility of dimers is limited, a dimer-based disordered structure is formed (state 3). As the temperature is elevated, the dimers' mobility becomes sufficient to form the striped network (state 4b), as this requires the lowest energy barriers corresponding to the dimer attachment to striped islands; the on-surface gas of monomers (state 4a) and the dense network (state 4c) are less accessible at these temperatures, even though

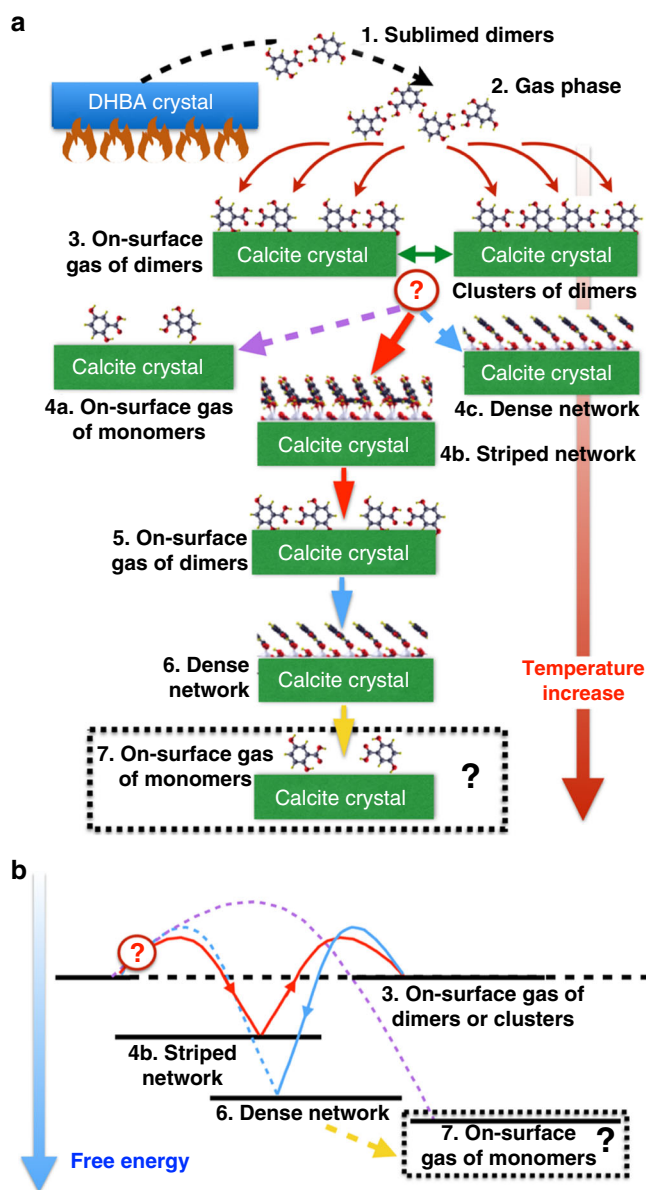


Fig. 8 Schematic summary diagrams illustrating all considered processes. The processes available to the system and the path taken are shown as a function of **a** temperature and **b** free energy. In **b** only on-surface states and processes as well as the minimum energy paths are shown schematically. In both panels solid arrowed lines correspond to the favorable transition paths, while dashed lines represent other possible processes, which are unlikely. Dimers sublimed from a DHBA powder are deposited on the calcite surface, held at a relatively low temperature, forming a structure composed of free dimers and their clusters, transitions 1 \rightarrow 2 \rightarrow 3. Next, the system chooses to form the striped islands (3 \rightarrow 4b) over other two paths available (on-surface monomers and dense islands) since the selected route corresponds to a higher effective rate (a lower energy barrier). Dissolution of the striped islands at higher temperature leads to mobile dimers, which diffuse towards existing dense islands and attach to them, contributing to their growth (4b \rightarrow 5 \rightarrow 6). We speculate that eventually, at even higher temperatures, the dense islands may decompose leading to the on-surface gas of monomers (6 \rightarrow 7), the most energetically favorable structure. Hence, over the whole transition path the free energy of the system decreases. (Images of structures used were adopted from ref. 17)

both structures have a lower free energy (Fig. 8b). The specific initial state 3 created in our experiments, an on-surface gas of dimers, triggered the specific evolution path for the DHBA molecules along the different networks, including the formation of metastable striped islands. As the temperature is increased further, dimers are able to detach from the striped islands, (transition 4B → 5). The dimers leave the striped network, diffuse, and attach to existing dense islands (5 → 6), as this requires even smaller barriers than for the detachment from the striped network. These low values stem from a “network-assisted” dimer dissociation, an effect induced by the proximity of the dense island to the approaching dimer. Thus, the island catalyzes the breaking of the dimer—another important ingredient for the specific sequence of structures observed. In this respect, we speculate that if the dimer dissociation was not assisted, the scenario would have been completely different, with the dense network not forming at all. Indeed, the required energy barrier to form this network would be comparable to the one necessary to dissociate dimers into monomers (1.35 eV), leading directly to the thermodynamically most stable phase of on-surface monomers (see Figs. 5 and 8b).

As the temperature is increased even further, the dense islands would decompose, and the on-surface gas of monomers would finally prevail (Fig. 8). However, the fact that monomers are not observed experimentally in the temperature range studied, indicates a rather high barrier for their formation on the surface.

Note that, as the barriers for all processes are relatively close, the striped-to-dense transition may even happen at a not-too-elevated (e.g., room) temperature, although in this case the process requires a considerable time (many hours, see Supplementary Movie 1)¹⁶.

Concluding, in this work we propose a novel route for creating a set of metastable molecular architectures on crystal surfaces. This is achieved by triggering a sequence of structural transformations entirely controlled by kinetics rather than thermodynamics. The first key feature of our approach is a judicious choice of the initial molecular state of the system, immediately after the deposition on the surface. The second is a controlled, stepwise heating procedure necessary to make the metastable networks accessible from the initial state first, and from one another in subsequent stages.

The feasibility of this route is demonstrated by an example of DHBA organic molecules deposited on an insulating calcite surface. Here, the initial state of the system is an on-surface gas of mostly DHBA dimers. Via a comprehensive theoretical analysis, we show that dimers (rather than monomers) trigger the specific structural transformation observed, due to the hierarchy of energy barriers connecting different molecular arrangements. The sequence of structures (disordered → ordered striped → ordered dense → disordered), is controlled by kinetics: at each relevant temperature interval, the kinetically most accessible structure is formed, selected on the basis of the lowest energy barriers, rather than of its thermodynamic stability. The observed structural path is associated with an increased thermodynamic stability of the whole system.

We believe that this study has a wide appeal since it demonstrates, by providing a detailed insight into the mechanisms of growth of molecular assemblies, the importance of the initial molecular state on the surface and the crucial role of kinetics. Accessing specific structural paths via kinetic control could significantly expand our abilities of realizing a wider variety of molecular motifs on metallic and insulating surfaces. This could represent an important step in designing molecular architectures on substrates, with a potential in the area of growth and structural transformations of organic molecular self-assemblies and in surface functionalization.

Methods

Computational methods. DFT calculations were mainly performed with the Quickstep code¹⁹ (within the CP2K package, <http://www.cp2k.org/>), that uses a mixed Gaussian and plane waves basis set, the Goedecker, Teter and Hutter (GTH) pseudopotentials²⁰ and a GGA-PBE²¹ exchange-correlation functional including a Grimme-D2 van der Waals interaction.²² We used a plane-wave basis energy cut-off of 600 Ry and the Γ point to sample the Brillouin-zone. In all calculations large enough supercells were considered to justify the latter approximation, e.g., 6×2 cell (in terms of the primitive calcite unit cell) measuring $3.03 \times 1.62 \text{ nm}^2$ was used to model the striped and dense networks. The calcite substrate was modeled with a periodically repeated slab of three layers, allowing a vacuum gap between the adsorbed ad-layer and the bottom layer of the slab above it of $\sim 30 \text{ \AA}$. Relaxations were considered completed when atomic forces were $< 0.02 \text{ eV/\AA}$. Only atoms belonging to the two uppermost top layers and all atoms of the molecules were allowed to relax. Atomic vibrations were calculated using the frozen-phonon method with the free energy obtained within the quasi-harmonic approximation.²³ Climbing image nudged elastic band (CI-NEB)^{24, 25} calculations were performed using overall between 9 and 14 replicas, including the initial and final states. Note that the appropriate vibrational analysis at the saddle points was not performed due to enormous cost and complexity of such calculations. Pre and postprocessing were done using the TETR/LEV00 package (<http://www.nms.kcl.ac.uk/lev.kantorovitch/codes/lev00/index.html>).

Experimental methods. Sample preparations and AFM measurements were carried out under ultrahigh vacuum conditions with a base pressure $< 10^{-10}$ mbar. Temperature-dependent high-resolution images were performed with a Scienta Omicron VT AFM XA operated in the frequency modulation mode following the procedure reported previously¹⁷. A Pt-100 sensor with an accuracy of $\pm K$ located at the sample holder stage was used to determine the temperatures stated in this article. The unknown temperature difference between sample holder stage and sample surface is estimated by the manufacturer to be less than 10 K. Optical quality calcite (CaCO_3) crystals were purchased from Korth Kristalle GmbH, Kiel, Germany and cleaved in situ to obtain less contaminated (10.4) surfaces. Sub-monolayers of DHBA molecules from Aldrich, Munich, Germany were deposited on the surface by heating a prior thoroughly outgassed home-built Knudsen cell to $67 \text{ }^\circ\text{C}$.

Data and code availability

The data that support the findings of this study are available from the corresponding author upon reasonable request.

Received: 3 January 2018 Accepted: 26 September 2018

Published online: 22 October 2018

References

1. Barth, J. V. Molecular architectonic on metal surfaces. *Annu. Rev. Phys. Chem.* **58**, 375–407 (2007).
2. Rosei, F. et al. Properties of large organic molecules on metal surfaces. *Prog. Surf. Sci.* **71**, 95–146 (2003).
3. Pawin, G., Wong, K. L., Kwon, K. Y. & Bartels, L. A homomolecular porous network at a Cu(111). *Surf. Sci.* **313**, 961–962 (2006).
4. Pawin, G. et al. A surface coordination network based on substrate-derived metal adatoms with local charge excess. *Angew. Chem. Int. Ed.* **47**, 8442–8445 (2008).
5. Phillips, A. G., Perdigo, L. M. A., Beton, P. H. & Champness, N. R. Tailoring pores for guest entrapment in a unimolecular surface self-assembled hydrogen bonded network. *Chem. Commun.* **46**, 2775–2777 (2010).
6. Böhringer, M. et al. Two-dimensional self-assembly of supramolecular clusters and chains. *Phys. Rev. Lett.* **83**, 324–327 (1999).
7. Abdurakhmanova, N. et al. Stereoselectivity and electrostatics in charge-transfer Mn- and Cs-TCNQ4 networks on Ag(100). *Nat. Commun.* **3**, 940 (2012).
8. Floris, A., Comisso, A. & De Vita, A. Fine-tuning the electrostatic properties of an alkali-linked organic adlayer on a metal substrate. *ACS Nano* **7**, 8059–8065 (2013).
9. Della Pia, A. et al. Anomalous coarsening driven by reversible charge transfer at metal–organic interfaces. *ACS Nano* **8**, 12356–12364 (2014).
10. Rahe, P. et al. Tuning molecular self-assembly on bulk insulator surfaces by anchoring of the organic building blocks. *Adv. Mater.* **25**, 3948–3956 (2013).
11. Kunstmann, T. et al. Dynamic force microscopy study of 3,4,9,10-perylenetetracarboxylic dianhydride on KBr(001). *Phys. Rev. B* **71**, 121403(R) (2005).
12. Nony, L. et al. Cu-TBPP and PTCDA molecules on insulating surfaces studied by ultra-high-vacuum non-contact AFM. *Nanotechnology* **15**, S91–S96 (2004).

13. Hauke, C. M. et al. Controlling molecular self-assembly on an insulating surface by rationally designing an efficient anchor functionality that maintains structural flexibility. *ACS Nano* **7**, 5491–5498 (2013).
14. Rahe, P., Lindner, R., Kittelmann, M., Nimmrich, M. & Kühnle, A. From dewetting to wetting molecular layers: C60 on CaCO₃(104) as a case study. *Phys. Chem. Chem. Phys.* **14**, 6544–6548 (2012).
15. Kittelmann, M. et al. Controlled activation of substrate templating in molecular self-assembly by deprotonation. *J. Phys. Chem. C* **117**, 23868–23874 (2013).
16. Kittelmann, M., Rahe, P., Gourdon, A. & Kühnle, A. Direct visualization of molecule deprotonation on an insulating surface. *ACS Nano* **6**, 7406–7411 (2012).
17. Paris, C. et al. Increasing the templating effect on a bulk insulator surface: from a kinetically trapped to a thermodynamically more stable structure. *J. Phys. Chem. C* **120**, 17546–17554 (2016).
18. Adam, M. S. et al. Stability and cooperativity of hydrogen bonds in dihydroxybenzoic acids. *New J. Chem.* **34**, 85–91 (2010).
19. VandeVondele, J. et al. Quickstep: fast and accurate density functional calculations using a mixed gaussian and plane waves approach. *Comput. Phys. Commun.* **167**, 103–128 (2005).
20. Goedecker, S., Teter, M. & Hutter, J. Separable dual-space Gaussian pseudopotentials. *Phys. Rev. B* **54**, 1703–1710 (1996).
21. Perdew, J. P., Burke, K. & Ernzerhof, M. Generalized gradient approximation made simple. *Phys. Rev. Lett.* **77**, 3865–3868 (1996).
22. Grimme, S. Semiempirical GGA-type density functional constructed with a long-range dispersion correction. *J. Comp. Chem.* **27**, 1787–1799 (2006).
23. Kantorovich, L. *Quantum Theory of the Solid State: An Introduction*. (Kluwer, London, 2004).
24. Jónsson, H., Mills, G. & Jacobsen, K. W. Nudged elastic band method for finding minimum energy paths of transitions, in *Classical and Quantum Dynamics in Condensed Phase Simulations*. (eds Berne, B. J., Ciccotti, G., & Coker, D. F.) Vol. 385 (World Scientific, Singapore, New Jersey, London, Hong Kong, 1998).
25. Henkelman, G. & Jonson, H. A climbing image nudged elastic band method finding saddle points and minimum energy paths. *J. Chem. Phys.* **113**, 9901–9904 (2000).

Acknowledgments

C.P. would like to thank the ACRTAS Marie Curie Initial Training Network (ITN) project for funding. Via our membership of the UK's HEC Materials Chemistry Consortium, which is funded by EPSRC (EP/L000202), this work used the ARCHER UK National Supercomputing Service (<http://www.archer.ac.uk>). Financial support from the EU through grant PAMS (seventh framework program GA 610446) is gratefully

acknowledged. S.A. is a recipient of a DFG-fellowship through the Excellence Initiative by the Graduate School Materials Science in Mainz (GSC 266). A.K. gratefully acknowledges funding from the Germany Research Foundation via grant KU1980/10-1.

Author contributions

C.P. performed all calculations; L.K., A.F., and C.P. planned and discussed the calculations strategy; S.A., J.N., and F.K. designed and performed the experiments; L.K., A.K., and A.F. wrote the manuscript with contributions from all authors, and all the authors discussed the results.

Additional information

Supplementary information accompanies this paper at <https://doi.org/10.1038/s42004-018-0069-0>.

Competing interests: The authors declare no competing interests.

Reprints and permission information is available online at <http://npg.nature.com/reprintsandpermissions/>

Publisher's note: Springer Nature remains neutral with regard to jurisdictional claims in published maps and institutional affiliations.



Open Access This article is licensed under a Creative Commons Attribution 4.0 International License, which permits use, sharing, adaptation, distribution and reproduction in any medium or format, as long as you give appropriate credit to the original author(s) and the source, provide a link to the Creative Commons license, and indicate if changes were made. The images or other third party material in this article are included in the article's Creative Commons license, unless indicated otherwise in a credit line to the material. If material is not included in the article's Creative Commons license and your intended use is not permitted by statutory regulation or exceeds the permitted use, you will need to obtain permission directly from the copyright holder. To view a copy of this license, visit <http://creativecommons.org/licenses/by/4.0/>.

© The Author(s) 2018